Roughness characteristics in aufeis morphology

Kazuto Ueno* and Masoud Farzaneh
NSERC/Hydro-Quebec/UQAC Industrial Chair on Atmospheric Icing of Power Network Equipment (CIGELE) and Canada Research Chair on Atmospheric Icing Engineering of Power Networks (INGIVRE), www.cigele.ca
Université du Québec à Chicoutimi, Chicoutimi, QC, Canada
*Email: kazuto.ueno@uqac.ca

Abstract: Aufeis (also referred to as icing, or as naleds in Russian) are spreading and thickening ice accretions that form in cold air when a shallow sheet of water flows over a cold surface and progressively freezes on it. Aufeis formation was simulated on a sloped planar aluminum surface subject to wind. An initial morphologies of aufeis appeared wavelike (or terraced), and its roughness spacing and height varied with slope and wind speed. This paper proposes a theoretical model to explain the roughness characteristics of the initial aufeis morphology. Water is introduced from the top of a plane set in a cold room, and the resulting supercooled water is driven by gravity and wind drag. In this model, ice grows from the water film by releasing latent heat to the air by convection and by heat conduction into an aluminum substrate beneath the ice sheet. The water and air boundary layers are simultaneously disturbed due to change in the ice shape and the disturbed water flow interacts with the air flow. Applying linear stability analysis on this air/water/ice/aluminum multi-phase system, the effects of the water supply rate, plane slope, and air stream velocity on the spacing and height of ice surface roughness were investigated. It was found that air shear stress disturbances at the water-air interface affect the convective heat transfer rate and the ice growth conditions.

1. INTRODUCTION

We consider a model of ice growth on an inclined aluminum plate supplied by water from the top. The current model is based on experiments by Streitz and Ettema for an initial aufeis formation on an inclined plane in a cold room [1]. The water flows as a thin sheet driven by gravity and wind drag. One side of the water film is a water-air interface and the other side is growing ice. The initial aufeis morphologies observed in the Streitz and Ettema experiments were wavelike (or terraced), and their spacing and height varied with plane slopes and wind speeds. For a given water supply rate, plane slope and air stream velocity, an initial aufeis morphology was investigated using linear stability analysis.

2. RESULTS

In this study, the effect of the interaction between air and water flows on the ice growth conditions is taken into account. In Figs. 1(a) and (b), air shear stress disturbances are considered in the solid lines, which is not the case for the dashed lines. If we neglect the effect of the air shear stress disturbances on the water-air interface, the shape of the water-air interface is not correctly predicted. As a result, the heat transfer coefficient at the water-air interface is erroneously estimated. Consequently, the amplification rate of the ice-water interface disturbance is overestimated. This result indicates that in order to evaluate the amplitude of the ice surface roughness, the amplification rate must be correctly evaluated without neglecting the interaction between air and water flows.

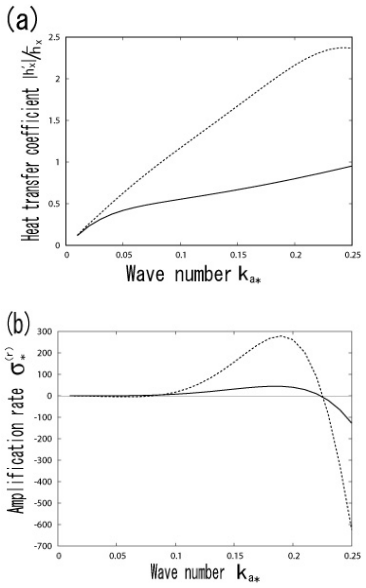

Figure 1: (a) The ratio of disturbed convective heat transfer coefficient to undisturbed one vs. dimensionless wave number. (b) Dimensionless amplification rate vs. dimensionless wave number. The solid line is the case with air shear stress disturbances. The dashed line is the case without air shear stress disturbances.

3. CONCLUSION

Using linear stability analysis, the roughness spacing and amplification rate of the ice-water interface were calculated for a given water supply rate, plane slope and air stream velocity. The major findings are follows: (1) The ice-water interface becomes unstable as the ice thickness increases and its characteristic wavelength is about 1 cm. (2) If the effect of air shear stress disturbances on the water-air interface is neglected, the magnitude of the disturbed heat transfer coefficient and the amplification rate of the ice-water interface disturbance are overestimated.

4. REFERENCES

[1] J. T. Streitz and R. Ettema, "Observations from an aufeis windtunnel," Cold Reg. Sci. Technol, vol. 34, pp. 85–96, 2002.

Roughness characteristics in aufeis morphology

Kazuto Ueno and Masoud Farzaneh
NSERC/Hydro-Quebec/UQAC Industrial Chair on Atmospheric Icing of Power Network Equipment (CIGELE) and Canada Research Chair on Atmospheric Icing Engineering of Power Networks (INGIVRE), www.cigele.ca
Université du Québec à Chicoutimi, Chicoutimi, QC, Canada

***Abstract*— Aufeis (also referred to as icing, or as naleds in Russian) are spreading and thickening ice accretions that form in cold air when a shallow sheet of water flows over a cold surface and progressively freezes on it. Aufeis formation was simulated on a sloped planar aluminum surface subject to wind. An initial morphologies of aufeis appeared wavelike (or terraced), and its roughness spacing and height varied with slope and wind speed. This paper proposes a theoretical model to explain the roughness characteristics of the initial aufeis morphology. Water is introduced from the top of a plane set in a cold room, and the resulting supercooled water is driven by gravity and wind drag. In this model, ice grows from the water film by releasing latent heat to the air by convection and by heat conduction into an aluminum substrate beneath the ice sheet. The water and air boundary layers are simultaneously disturbed due to change in the ice shape and the disturbed water flow interacts with the air flow. Applying linear stability analysis on this air/water/ice/aluminum multi-phase system, the effects of the water supply rate, plane slope, and air stream velocity on the spacing and height of ice surface roughness were investigated. It was found that air shear stress disturbances at the water-air interface affect the convective heat transfer rate and the ice growth conditions.**

Keywords-Aufeis; Supercooled water; Linear stability analysis

I. INTRODUCTION

We consider a model of ice growth on an inclined aluminum plate supplied by water from the top, as shown in Fig. 1. The current model is based on the experiments by Streitz and Ettema about an initial aufeis formation on an inclined plane in a cold room [1]. In the physical model, water flows as a thin film driven by gravity and wind drag. One side of the water film is a water-air interface and the other side is growing ice. The initial aufeis morphologies observed in the Streitz and Ettema experiments were wavelike (or terraced), and their spacing and height varied with various plane slopes and wind speeds. In Fig. 1, x is the position along the inclined plane measured from the top, and y is the position measured from a flat ice-water interface. The water supply rate per width was the same as in Streitz and Ettema experiments. θ is the angle of the

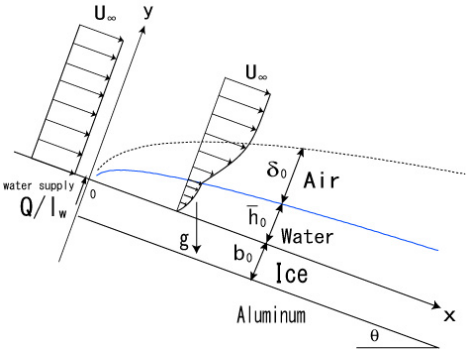

Figure1. Schematic view of model and coordinate system.

inclined plane with respect to the horizontal. A steady air and water flows is parallel to the x axis. u_∞ is the free stream velocity. δ_0, $\bar{h}_0$ and b_0 are the thickness of air boundary layer, water layer and ice, respectively. The values $Q/l_w = 1692$[(ml/h)/cm] [1], $\theta = \pi/18$ and $u_\infty = 20$ m/s are used throughout this paper. An initial aufeis morphology was investigated using linear stability analysis.

II. GOVERNING EQUATIONS

The equations governing momentum and heat in the air region are

$$\frac{\partial u_a}{\partial t} + u_a \frac{\partial u_a}{\partial x} + \mathrm{v}_a \frac{\partial u_a}{\partial y} = -\frac{1}{\rho_a}\frac{\partial p_a}{\partial x} + \nu_a\left(\frac{\partial^2 u_a}{\partial x^2} + \frac{\partial^2 u_a}{\partial y^2}\right), \quad (1)$$

$$\frac{\partial \mathrm{v}_a}{\partial t} + u_a \frac{\partial \mathrm{v}_a}{\partial x} + \mathrm{v}_a \frac{\partial \mathrm{v}_a}{\partial y} = -\frac{1}{\rho_a}\frac{\partial p_a}{\partial y} + \nu_a\left(\frac{\partial^2 \mathrm{v}_a}{\partial x^2} + \frac{\partial^2 \mathrm{v}_a}{\partial y^2}\right), \quad (2)$$

$$\frac{\partial u_a}{\partial x} + \frac{\partial \mathrm{v}_a}{\partial y} = 0, \quad (3)$$

$$\frac{\partial T_a}{\partial t} + u_a \frac{\partial T_a}{\partial x} + \mathrm{v}_a \frac{\partial T_a}{\partial y} = \kappa_a\left(\frac{\partial^2 T_a}{\partial x^2} + \frac{\partial^2 T_a}{\partial y^2}\right), \quad (4)$$

where u_a, v_a are air flow velocities, p_a and T_a the air pressure and temperature, and ρ_a, ν_a and κ_a are the density, kinematic viscosity and thermal diffusivity of air. The equations governing momentum and heat in the water region are

$$\frac{\partial u_l}{\partial t} + u_l \frac{\partial u_l}{\partial x} + \mathrm{v}_l \frac{\partial u_l}{\partial y} = -\frac{1}{\rho_l}\frac{\partial p_l}{\partial x} + \nu_l\left(\frac{\partial^2 u_l}{\partial x^2} + \frac{\partial^2 u_l}{\partial y^2}\right) + g\sin\theta, \quad (5)$$

$$\frac{\partial \mathrm{v}_l}{\partial t}+u_l\frac{\partial \mathrm{v}_l}{\partial x}+\mathrm{v}_l\frac{\partial \mathrm{v}_l}{\partial y}=-\frac{1}{\rho_l}\frac{\partial p_l}{\partial y}+\nu_l\left(\frac{\partial^2 \mathrm{v}_l}{\partial x^2}+\frac{\partial^2 \mathrm{v}_l}{\partial y^2}\right)-g\cos\theta, \quad (6)$$

$$\frac{\partial u_l}{\partial x}+\frac{\partial \mathrm{v}_l}{\partial y}=0, \quad (7)$$

$$\frac{\partial T_l}{\partial t}+u_l\frac{\partial T_l}{\partial x}+\mathrm{v}_l\frac{\partial T_l}{\partial y}=\kappa_l\left(\frac{\partial^2 T_l}{\partial x^2}+\frac{\partial^2 T_l}{\partial y^2}\right), \quad (8)$$

where u_l, v_l are water flow velocities, p_l and T_l are the water pressure and temperature, and ρ_l, ν_l and κ_l are the density, kinematic viscosity and thermal diffusivity of water, g is the gravitational acceleration and θ is the plane angle. The temperature T_s in the ice region is governed by

$$\frac{\partial T_s}{\partial t}=\kappa_s\left(\frac{\partial^2 T_s}{\partial x^2}+\frac{\partial^2 T_s}{\partial y^2}\right). \quad (9)$$

At the ice-water interface, $y=\zeta$, the no-slip condition is imposed:

$$u_l\,|_{y=\zeta}=0,\ \ \mathrm{v}_l\,|_{y=\zeta}=0. \quad (10)$$

At the water-air interface, $y=\xi$, the kinematic condition is

$$\frac{\partial \xi}{\partial t}+u_l\,|_{y=\xi}\frac{\partial \xi}{\partial x}=\mathrm{v}_l\,|_{y=\xi}. \quad (11)$$

Velocity, normal and tangential stresses are continuous across the water-air interface:

$$u_l\,|_{y=\xi}=u_a\,|_{y=\xi},\qquad \mathrm{v}_l\,|_{y=\xi}=\mathrm{v}_a\,|_{y=\xi}, \quad (12)$$

$$\mu_l\left(\left.\frac{\partial u_l}{\partial y}\right|_{y=\xi}+\left.\frac{\partial \mathrm{v}_l}{\partial x}\right|_{y=\xi}\right)=\mu_a\left(\left.\frac{\partial u_a}{\partial y}\right|_{y=\xi}+\left.\frac{\partial \mathrm{v}_a}{\partial x}\right|_{y=\xi}\right), \quad (13)$$

$$-p_a\,|_{y=\xi}+2\mu_a\left.\frac{\partial \mathrm{v}_a}{\partial y}\right|_{y=\xi}-\left(-p_l\,|_{y=\xi}+2\mu_l\left.\frac{\partial \mathrm{v}_l}{\partial y}\right|_{y=\xi}\right)=-\gamma\frac{\partial^2 \xi}{\partial x^2}, \quad (14)$$

where μ_l, μ_a are the viscosities of water and air, and γ is the surface tension of the water-air interface. The continuity of temperature and heat flux at the ice-water interface, $y=\zeta$, is

$$T_l\,|_{y=\zeta}=T_s\,|_{y=\zeta}=T_i, \quad (15)$$

$$L\left(\overline{V}+\frac{\partial \zeta}{\partial t}\right)=K_s\left.\frac{\partial T_s}{\partial y}\right|_{y=\zeta}-K_l\left.\frac{\partial T_l}{\partial y}\right|_{y=\zeta}, \quad (16)$$

where the temperature at the ice-water interface, T_i is an unknown to be determined because the interface is subject to the shearing water flow, L is the latent heat per unit volume, $\overline{V}$ is the undisturbed ice growth rate, K_s and K_l are thermal conductivities of ice and water, respectively. The continuity of temperature and heat flux at the water-air interface, $y=\xi$, is

$$T_l\,|_{y=\xi}=T_a\,|_{y=\xi}=T_{la}, \quad (17)$$

$$-K_l\left.\frac{\partial T_l}{\partial y}\right|_{y=\xi}=-K_a\left.\frac{\partial T_a}{\partial y}\right|_{y=\xi}, \quad (18)$$

where T_{la} is the temperature at the water-air interface, and K_a is the thermal conductivity of air. Finally, as $y\to\infty$ the velocities and temperature asymptote to their far-field values:

$$u_a\,|_{y=\infty}=u_\infty,\ \ \mathrm{v}_a\,|_{y=\infty}=0,\ \ T_a\,|_{y=\infty}=T_\infty. \quad (19)$$

III. LINEAR STABILITY ANALYSIS

The field variables are decomposed into undisturbed and disturbed parts, as follows:

$$\begin{pmatrix}\zeta\\ \xi\\ \psi_a\\ \psi_l\\ p_a\\ p_l\\ T_a\\ T_l\\ T_s\end{pmatrix}=\begin{pmatrix}0\\ \overline{h}_0\\ u_\infty\delta_0\overline{F}_a\\ u_{la}\overline{h}_0\overline{F}_l\\ \overline{p}_a\\ \overline{p}_l\\ \overline{T}_a\\ \overline{T}_l\\ \overline{T}_s\end{pmatrix}+\begin{pmatrix}\zeta_k\\ \xi_k\\ u_\infty f_a(\eta)\xi_k\\ u_{la}f_l(y_*)\zeta_k\\ (\rho_a u_\infty^2/\delta_0)g_a(\eta)\xi_k\\ (\rho_l u_{la}^2/\overline{h}_0)g_l(y_*)\zeta_k\\ H_a(\eta)\overline{G}_a\xi_k\\ H_l(y_*)\overline{G}_l\zeta_k\\ H_s(y_*)\overline{G}_l\zeta_k\end{pmatrix}\exp[\sigma t+ikx], \quad (20)$$

The disturbed part is of typical normal mode form. In (20) $\sigma=\sigma_r+i\sigma_i$ is complex, where σ_r is the growth rate of the disturbance and σ_i is the oscillation frequency, k is the wave number of the disturbance along the x direction. $\eta=(y-\overline{h}_0)/\delta_0$, $\delta_0=(2\nu_a x/u_\infty)^{1/2}$, $y_*=y/\overline{h}_0$, $\overline{G}_a\equiv-\partial\overline{T}_a/\partial y\big|_{y=\overline{h}_0}$, $\overline{G}_l\equiv-\partial\overline{T}_l/\partial y\big|_{y=0}$, and (ζ_k , ξ_k , f_a , f_l , g_a , g_l , H_a , H_l , H_s) are amplitudes of each disturbance. u_∞ and u_{la} are the free stream velocity and the surface velocity of the water film, respectively. Substituting ψ_a, T_a, ψ_l, T_l into (1), (2), (4) and (5), (6), (8), a set of dimensionless differential equations for the undisturbed part $\overline{F}_a$, $\overline{T}_{a*}=(\overline{T}_a-T_\infty)/(T_{la}-T_\infty)$, $\overline{u}_{l*}\equiv\overline{u}_l/u_{la}=d\overline{F}_l/dy_*$, $\overline{T}_{l*}=(\overline{T}_l-T_{sl})/(T_{sl}-T_{la})$ and those for the disturbed part f_a , H_a , f_l , H_l are obtained:

$$\frac{d^3\overline{F}_a}{d\eta^3}=-\overline{F}_a\frac{d^2\overline{F}_a}{d\eta^2},\qquad \frac{d^2\overline{T}_{a*}}{d\eta^2}=-\mathrm{Pr}_a\overline{F}_a\frac{d\overline{T}_{a*}}{d\eta}, \quad (21)$$

$$\frac{d^2\overline{u}_{l*}}{dy_*^2}=-\frac{g\overline{h}_0^2\sin\theta}{\nu_l u_{la}},\qquad \frac{d^2\overline{T}_{l*}}{dy_*^2}=0, \quad (22)$$

$$\frac{d^4 f_a}{d\eta^4}=-\overline{F}_a\frac{d^3 f_a}{d\eta^3}+\left\{2k_{a*}^2+(2-ik_{a*}\mathrm{Re}_a)\frac{d\overline{F}_a}{d\eta}\right\}\frac{d^2 f_a}{d\eta^2}$$
$$+\left\{k_{a*}^2\left(\overline{F}_a+2\eta\frac{d\overline{F}_a}{d\eta}-\frac{d^2\overline{F}_a}{d\eta^2}\right)\right\}\frac{df_a}{d\eta}-\left\{k_{a*}^4+ik_{a*}\mathrm{Re}_a\left(k_{a*}^2\frac{d\overline{F}_a}{d\eta}+\frac{d^3\overline{F}_a}{d\eta^3}\right)\right\}f_a \quad (23)$$

$$\frac{d^2(\overline{G}_{a*}H_a)}{d\eta^2} = -\mathrm{Pr}_a \overline{F}_a \frac{d(\overline{G}_{a*}H_a)}{d\eta} + \left\{k_{a*}^2 + \mathrm{Pr}_a\left(-1 + ik_{a*}\mathrm{Re}_a \frac{d\overline{F}_a}{d\eta}\right)\right\}(\overline{G}_{a*}H_a) - ik_{a*}\mathrm{Pr}_a \mathrm{Re}_a \frac{d\overline{T}_{a*}}{d\eta} f_a, \quad (24)$$

$$\frac{d^4 f_l}{dy_*^4} = \left(2k_{l*}^2 + ik_{l*}\mathrm{Re}_l \overline{u}_{l*}\right)\frac{d^2 f_l}{dy_*^2} - \left\{k_{l*}^4 + ik_{l*}\mathrm{Re}_l\left(k_{l*}^2 \overline{u}_{l*} + \frac{d^2\overline{u}_{l*}}{dy_*^2}\right)\right\} f_l, \quad (25)$$

$$\frac{d^2(\overline{G}_{l*}H_l)}{d\eta^2} = \left(k_{l*}^2 + ik_{l*}Pe_l\overline{u}_{l*}\right)(\overline{G}_{l*}H_l) - ik_{l*}Pe_l \frac{d\overline{T}_{l*}}{dy_*} f_l, \quad (26)$$

where $\overline{G}_{a*} \equiv -d\overline{T}_{a*}/d\eta\big|_{\eta=0}$ and $\overline{G}_{l*} \equiv -d\overline{T}_{l*}/dy_*\big|_{y_*=0}$. $\mathrm{Re}_a = u_\infty \delta_0/\nu_a$, $\mathrm{Re}_l = u_{la}\overline{h}_0/\nu_l$ and $\mathrm{Pr}_a = \nu_a/\kappa_a$, $\mathrm{Pr}_l = \nu_l/\kappa_l$ are the Reynolds numbers and the Prandtl numbers of air and water, $k_{a*} = k\delta_0$ and $k_{l*} = k\overline{h}_0$ are dimensionless wave numbers.

From (10)-(19), the boundary conditions for $\overline{F}_a, \overline{T}_{a*}, f_a, H_a, f_l, H_l$ can be expressed as:

$$\frac{d\overline{F}_a}{d\eta}\bigg|_{\eta=0} = \frac{u_{la}}{u_\infty}, \quad \overline{F}_a\big|_{\eta=0} = 0, \quad \frac{d\overline{F}_a}{d\eta}\bigg|_{\eta=\infty} = 1,$$
$$\overline{T}_{a*}\big|_{\eta=0} = 1, \quad \overline{T}_{a*}\big|_{\eta=\infty} = 0, \quad (27)$$

$$\frac{df_a}{d\eta}\bigg|_{\eta=0} = \left(-1 + \frac{\mu_a}{\mu_l}\right)\frac{d^2\overline{F}_a}{d\eta^2}\bigg|_{\eta=0} - \frac{\delta_0}{\overline{h}_0}\frac{u_{la}}{u_\infty}\frac{df_l}{dy_*}\bigg|_{y_*=1} \Big/ f_l\big|_{y_*=1},$$

$$f_a\big|_{\eta=0} = -\frac{u_{la}}{u_\infty} f_l\big|_{y_*=1}, \quad \frac{df_a}{d\eta}\bigg|_{\eta=\infty} = 0, \quad f_a\big|_{\eta=\infty} = 0, \quad (28)$$

$$H_a\big|_{\eta=0} = 1, \quad H_a\big|_{\eta=\infty} = 0, \quad (29)$$

$$\frac{df_l}{dy_*}\bigg|_{y_*=0} + \frac{d\overline{u}_{l*}}{dy_*}\bigg|_{y_*=0} = 0, \quad f_l\big|_{y_*=0} = 0,$$
$$\frac{d^2 f_l}{dy_*^2}\bigg|_{y_*=1} + \left(k_{l*}^2 - \frac{d^2\overline{u}_{l*}}{dy_*^2}\bigg|_{y_*=1} + \Sigma_a\right) f_l\big|_{y_*=1} = 0,$$
$$\frac{d^3 f_l}{dy_*^3}\bigg|_{y_*=1} - \left(3k_{l*}^2 + ik_{l*}\mathrm{Re}_l\right)\frac{df_l}{dy_*}\bigg|_{y_*=1}$$
$$+ ik_{l*}\mathrm{Re}_l\left(\frac{d\overline{u}_{l*}}{dy_*}\bigg|_{y_*=1} + \frac{\cos\theta}{Fr^2} + We k_{l*}^2 + \Pi_a\right) f_l\big|_{y_*=1} = 0, \quad (30)$$

$$H_l\big|_{y_*=1} + f_l\big|_{y_*=1} = 0, \quad \frac{dH_l}{dy_*}\bigg|_{y_*=1} - \frac{\overline{h}_0}{\delta_0}\left(-\frac{dH_a}{d\eta}\bigg|_{\eta=0}\right) f_l\big|_{y_*=1} = 0, \quad (31)$$

where

$$\Sigma_a = \frac{\mu_a}{\mu_l}\frac{u_\infty}{u_{la}}\left(\frac{\overline{h}_0}{\delta_0}\right)^2\left(\frac{d^2 f_a}{d\eta^2}\bigg|_{\eta=0} + k_{a*}^2 f_a\big|_{\eta=0}\right), \quad (32)$$

$$\Pi_a = -\frac{\rho_a}{\rho_l}\left(\frac{u_\infty}{u_{la}}\right)^2 \frac{\overline{h}_0}{\delta_0}\frac{1 + ik_{a*}\mathrm{Re}_a}{1 + (k_{a*}\mathrm{Re}_a)^2}$$
$$\times\left[\frac{d^3 f_a}{d\eta^3}\bigg|_{\eta=0} - \left\{3k_{a*}^2 + (-1 + ik_{a*}\mathrm{Re}_a)\frac{d\overline{F}_a}{d\eta}\bigg|_{\eta=0}\right\}\frac{df_a}{d\eta}\bigg|_{\eta=0} + ik_{a*}\mathrm{Re}_a\frac{d^2\overline{F}_a}{d\eta^2}\bigg|_{\eta=0} f_a\big|_{\eta=0}\right], \quad (33)$$

$Fr = u_{la}/(g\overline{h}_0)^{1/2}$ is the Froude number and $We = \gamma/(\rho_l u_{la}^2 \overline{h}_0)$ is the Weber number. We refer to Σ_a and Π_a as the tangential and normal air shear stress disturbances, respectively, thorough which the disturbed part of the water flow is affected by the air flow. The undisturbed velocity and temperature in the water film are

$$\overline{u}_{l*} = -\frac{g\overline{h}_0^2 \sin\theta}{2\nu_l u_{la}} y_*^2 + \left(\frac{g\overline{h}_0^2 \sin\theta}{\nu_l u_{la}} + \frac{\mu_a u_\infty \overline{h}_0}{\mu_l u_{la}\delta_0}\frac{d^2\overline{F}_a}{d\eta^2}\bigg|_{\eta=0}\right) y_*, \quad (34)$$

$$\overline{T}_{l*} = -y_*. \quad (35)$$

The volumetric water flow rate per width, Q/l_w, can be expressed as

$$Q/l_w = \frac{g\sin\theta}{3\nu_l}\overline{h}_0^3 + \frac{\mu_a u_\infty}{2\mu_l\delta_0}\frac{d^2\overline{F}_a}{d\eta^2}\bigg|_{\eta=0}\overline{h}_0^2, \quad (36)$$

Finally, the dimensionless amplification rate, $\sigma_*^{(r)} \equiv \sigma^{(r)}/(K_a\overline{G}_a/L\overline{h}_0)$, and the dimensionless phase velocity, $\mathrm{v}_{p*} \equiv -\sigma^{(i)}/(kK_a\overline{G}_a/L)$, for the disturbance of the ice-water interface are as follows:

$$\sigma_*^{(r)} = -\frac{dH_l^{(r)}}{dy_*}\bigg|_{y_*=0} + K_l^s k_{l*}\frac{\cosh(k_{l*}b_0/\overline{h}_0)}{\sinh(k_{l*}b_0/\overline{h}_0)}\left(-G_l^s + H_l^{(r)}\big|_{y_*=0} - 1\right), \quad (37)$$

$$\mathrm{v}_{p*} = -\frac{1}{k_{l*}}\left(-\frac{dH_l^{(i)}}{dy_*}\bigg|_{y_*=0} + K_l^s k_{l*}\frac{\cosh(k_{l*}b_0/\overline{h}_0)}{\sinh(k_{l*}b_0/\overline{h}_0)}H_l^{(i)}\big|_{y_*=0}\right), \quad (38)$$

where $K_l^s = K_s/K_l$ is the ratio of the thermal conductivity of ice to that of water, $G_l^s \equiv \overline{G}_s/\overline{G}_l$ is the ratio of the undisturbed temperature gradient at the ice-water interface in ice to that in water. $H_l^{(r)}$ and $H_l^{(i)}$ are the real and imaginary parts of H_l. When the thickness of ice grown on the planar aluminum substrate satisfies the condition $b_0 >> (K_s/K_{\mathrm{sub}})l_{\mathrm{sub}}$ and the other side of surface of the aluminum substrate is exposed to ambient cold air, G_l^s can be approximated as $G_l^s = (K_l/K_a)(\delta_0/b_0)$, where K_{sub} and l_{sub} are the thermal conductivity and thickness of the aluminum plate [2]. The undisturbed ice growth rate is given by

$db_0/dt = (K_s/L)(T_{sl} - T_{\mathrm{sub}})/b_0 + (K_a/L)(T_{sl} - T_\infty)\overline{G}_{a*}/\delta_0$, from which the ice thickness b_0 is determined [2].

VI. Results

Fig. 2 shows the dimensionless amplification rate $\sigma_*^{(r)}$ versus the dimensionless wave number k_{a*}. In the

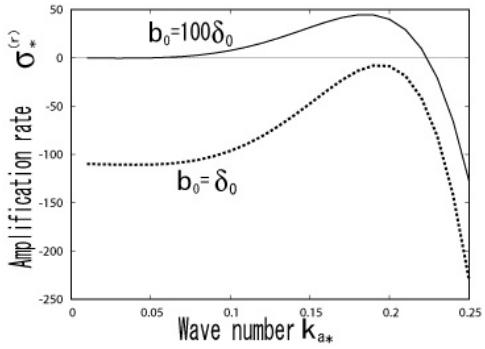

Figure 2. Dimensionless amplification rate $\sigma_*^{(r)}$ vs. dimensionless wave number k_{a*}.

case of $b_0 = 100\delta_0$, the ice-water interface disturbance becomes unstable and $\sigma_*^{(r)}$ acquires a maximum value at $k_{a*} = 0.18$. The corresponding wavelength of ice surface roughness is $\lambda = 2\pi\delta_0 / k_{a*} =$ 1.26 cm for $\delta_0 = 3.61\times10^{-4}$ m, and the ice-water interface disturbance moves upwards at a speed of $|\mathrm{v}_p| = 283\overline{V}$. On the other hand, in the case of $b_0 = \delta_0$, $\sigma_*^{(r)}$ is negative for all wave numbers, which means that an ice-water interface disturbance diminishes with time. Figs. 3 (a) and (b) show the ratio of the disturbed convective heat transfer coefficient to the undisturbed one, $|h_x'|/\overline{h}_x$, and $\sigma_*^{(r)}$ against the dimensionless wave number k_{a*}, respectively. In these figures, the solid lines take into account the effect of the tangential and normal air shear stress disturbances on the water-air interface, while the dashed lines do not consider them.

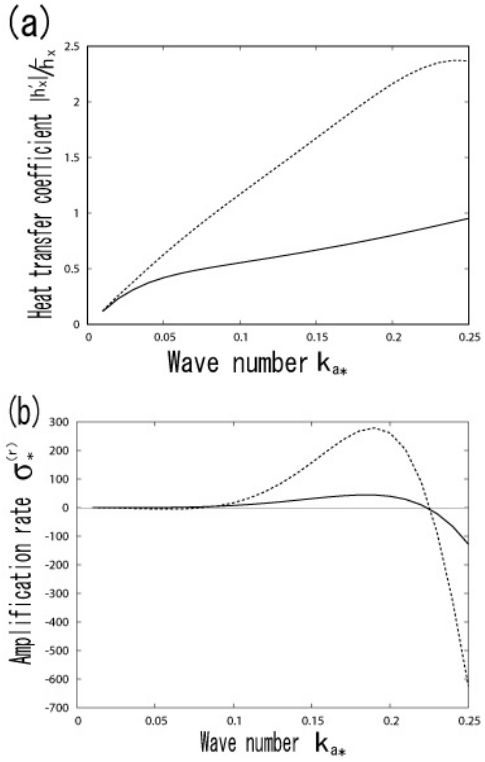

Figure 3. (a) The ratio of disturbed convective heat transfer coefficient to undisturbed one, $|h_x'|/\overline{h}_x$ vs. dimensionless wave number k_{a*} for $b_0 = 100\delta_0$. (b) $\sigma_*^{(r)}$ vs. k_{a*}. The solid line is the case with air shear stress disturbances. The dashed line is the case without air shear stress disturbances.

V. Conclusions

Using linear stability analysis, the roughness spacing and amplification rate of the ice-water interface were calculated for a given water supply rate, plane slope and air stream velocity. The major findings are follows: (1) The ice-water interface becomes unstable as ice thickness increases and its characteristic wavelength is about 1 cm. (2) If the effect of air shear stress disturbances on the water-air interface is neglected, the magnitude of the disturbed heat transfer coefficient and the amplification rate of the ice-water interface disturbance are overestimated.

Acknowledgment

This study was carried out within the framework of the NSERC/Hydro-Québec/UQAC Industrial Chair on Atmospheric Icing of Power Network Equipment (CIGELE) and the Canada Research Chair on Engineering of Power Network Atmospheric Icing (INGIVRE) at the Université du Québec à Chicoutimi. The authors would like to thank all CIGELE partners (Hydro-Quebec, Hydro One, Réseau Transport d'Electricite (RTE) and Electricité de France (EDF), Alcan Cable, K-Line Insulators, Tyco Electronics, Dual-ADE, and FUQAC) whose financial support made this research possible.

References

[1] J. T. Streitz and R. Ettema, "Observations from an aufeis windtunnel," Cold Reg. Sci. Technol, vol. 34, pp. 85–96, 2002.

[2] K. Ueno, M. Farzaneh, S. Yamaguchi, and H. Tsuji, "Numerical and experimental verification of a theoretical model of ripple formation in ice growth under supercooled water film flow," Fluid Dynamics Research, vol. 42, 025508, 27pp, 2010.